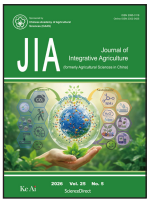
Journal of Integrative Agriculture 2026, 25(5): 2077–2092

KeAi CHINESE ROOTS GLOBAL IMPACT

Available online at ScienceDirect

Journal of Integrative Agriculture



RESEARCH ARTICLE

Low-phosphorus stress induces *GmSTOP1-3*-mediated organic acid exudation to recruit phosphate-solubilizing bacteria for organic phosphorus mineralization in soybean rhizosphere

Qianqian Chen[1, 2, 3, 5], Xing Lu[1, 3], Guoxuan Liu[1, 3], Tianqi Wang[1, 3], Huiying Zhou[1, 3], Jihui Tian[4], Qing Yao[5], Jinming He[2], Jiang Tian[1, 3#], Cuiyue Liang[1, 3#]

[1] *Root Biology Center, State Key Laboratory for Conservation and Utilization of Subtropical Agro-Bioresources, College of Natural Resources and Environment, South China Agricultural University, Guangzhou 510642, China*

[2] *Guangdong Provincial Key Laboratory of Utilization and Conservation of Food and Medicinal Resources in Northern Region, School of Biology and Agriculture, Shaoguan University, Shaoguan 512005, China*

[3] *Guangdong Engineering Technology Research Center of Low Carbon Agricultural Green Inputs, South China Agricultural University, Guangzhou 510642, China*

[4] *College of Natural Resources and Environment, South China Agricultural University, Guangzhou 510642, China*

[5] *Guangdong Province Key Laboratory of Microbial Signals and Disease Control/Guangdong Engineering Research Center for Litchi, College of Horticulture, South China Agricultural University, Guangzhou 510642, China*

Highlights

- Expression of *GmSTOP1-3* is up-regulated by phosphate starvation in soybean roots.
- *GmSTOP1-3* regulates root organic acid exudation and facilitates soil P utilization.
- *GmSTOP1-3*-mediated organic acid exudation recruits phosphate-solubilizing bacteria.

Abstract

Root exudates serve a vital function in recruiting beneficial phosphate-solubilizing bacteria (PSB), thereby enhancing plant adaptation to phosphorus (P) deficiency. The C2H2-type zinc finger transcription factor STOP1 (sensitive to proton rhizotoxicity 1) regulates root organic acid (OA) exudation in plants. However, the impact of STOP1-regulated root OA exudation on rhizosphere microbial composition remains unexplored. This study revealed enhanced vegetation properties of soybean with higher P content in P-rich soils, while rhizosphere organic acid concentrations were elevated in P-poor soils. The soybean genotype YC03-3 in P-deficient soils specifically recruited three PSB in acid soils: Gammaproteobacteria_Incertae_Sedis, KF_JG30_C25, and Solirubrobacterales. These PSB abundances correlated positively with rhizosphere oxalate and citrate concentrations. Under P-sufficient conditions, *GmSTOP1-3* overexpression in soybean plants increased oxalate and citrate exudation compared to YCO3-3 wild type (WT), leading to preferential colonization by the same three PSB species naturally present in P-deficient WT rhizosphere. The population dynamics of these PSB demonstrated strong positive correlations with the abundance of key genes involved in P cycling, particularly those governing acid/alkaline phosphatase activities and organic-P mineralization. Given the phosphate starvation-enhanced expression pattern of *GmSTOP1-3*, the findings indicate that specific PSB recruitment for organic-P remobilization in soybean rhizosphere depends on *GmSTOP1-3*-mediated oxalate and citrate exudation in P-deficient acid soils. This research establishes *GmSTOP1-3* as a crucial regulator of rhizosphere microbiome assembly and P-acquisition efficiency in acid soils.

Keywords: organic acid, phosphorus-cycling genes, phosphorus fractions, transcription factor, phosphatase activity

Received 1 April 2025; Received in revised form 1 June 2025; Accepted 1 June 2025; Available online 21 August 2025

Qianqian Chen, Mobile: +86-15915704184, E-mail: chenqq@scau.edu.cn; #Correspondence Jiang Tian, E-mail: jtian@scau.edu.cn; Cuiyue Liang, Mobile: +86-13570467247, E-mail: liangcy@scau.edu.cn

© 2026 CAAS. Publishing services by Elsevier B.V. on behalf of KeAi Communications Co. Ltd. This is an open access article under the CC BY-NC-ND license (http://creativecommons.org/licenses/by-nc-nd/4.0/). Peer review under responsibility of Editorial Board of *Journal of Integrative Agriculture*.
doi: 10.1016/j.jia.2025.08.015

1. Introduction

Phosphorus (P) is an essential macronutrient for plant growth and a primary limiting factor in acid soil (Vance *et al.* 2003). The application of P fertilizers represents a crucial approach to maintaining high crop yield (Herrera-Estrella and Lopez-Arredondo 2016). However, applied P fertilizers are predominantly adsorbed by Al/Fe oxides and organic complexes, forming insoluble P compounds (Shen *et al.* 2011; Chen *et al.* 2022; Zou *et al.* 2022). To optimize the utilization of legacy P, plants have evolved various strategies, known as Pi-starvation responses, including reconstruction of root morphology and architecture, induction of high-affinity Pi transporters, increased root exudation of organic acids and acid phosphatases, and symbiotic interaction with beneficial microbes (Mo *et al.* 2022; Li *et al.* 2024; Yang *et al.* 2024).

Enhanced organic acid exudation represents a significant strategy for plants to utilize soil insoluble P resources (Chen and Liao 2016; Peng *et al.* 2018; Lambers 2022; Li *et al.* 2023). Increased root organic exudation under P-deficiency has been documented in soybean (*Glycine max*), cowpea (*Vigna unguiculata*), maize (*Zea mays*), wheat (*Triticum aestivum*), Arabidopsis (*Arabidopsis thaliana*) and chickpea (*Cicer arietinum*) (Nwoke *et al.* 2008; Carvalhais *et al.* 2011; Pang *et al.* 2018; Peng *et al.* 2018; Xu *et al.* 2019; Gomez-Zepeda *et al.* 2021). Root-exudated organic acids directly remobilize sparingly soluble P resources, as demonstrated in soybean with enhanced Ca-P solubilization by malate (Peng *et al.* 2018), and in chickpea (*C. arietinum*) with enhanced Fe-P ($FePO_4$) remobilization by carboxylates (acetate, citrate, malate and malonate) (Pang *et al.* 2018). Additionally, root-exuded organic acids indirectly influence plant P-foraging by shaping specific phosphate-solubilizing bacteria (PSB) communities. Oxalate influences the abundance of *phoD*-harboring *Pseudomonas* and *Bacillus* in the lemon tree rhizosphere, subsequently altering soil P fractions (Wang *et al.* 2023). Similarly, root organic acid exudation of maize correlates positively with the relative abundances of *Streptomyces* (Zhang *et al.* 2023), which transform insoluble phosphorus into utilizable forms through the release of organic acid, H^+, and phosphatases (Aallam *et al.* 2021; Sadeghi *et al.* 2024).

The Pi starvation responses are regulated by multiple transcription factors. The PHR family members contribute to metabolic and developmental adaptations during P-deficiency, while also influencing plant–microbe interactions (Isidra-Arellano *et al.* 2021; Shi *et al.* 2021; Paries and Gutjahr 2023; Liu J P *et al.* 2024; Yang *et al.* 2024). Recent research indicates that *OsPHR2* enhanced the growth of *Pseudomonas* sp. in transgenic rice rhizosphere by increasing root exudation of succinic acid and methylmalonic acid (Liu J P *et al.* 2024). This finding demonstrates the role of plant Pi starvation responses in modifying rhizosphere bacterial communities. In addition to PHR1 transcription factors, the C2H2-type zinc finger transcription factor STOP1 (sensitive to proton rhizotoxicity 1) serves as a crucial regulator in plant root adaptation to P deficiency (Balzergue *et al.* 2017; Godon *et al.* 2019; Li and Tian 2023; Liu *et al.* 2025). Research has established that STOP1 facilitates plant root organic acid exudation by regulating the expression of *aluminum activated malate transporter1* (*ALMT1*) and *multidrug and toxic compound extrusion* (*MATE*) (Liu *et al.* 2009, 2025). Recent findings demonstrate that Pi-starvation enhanced soybean *GmSTOP1-3* regulated soybean root citrate exudation through direct control of *MATE2/13* genes (Liu *et al.* 2025). Given the established role of organic acid in shaping plant rhizosphere microorganisms, STOP1 potentially functions as a significant regulator in bacterial community reconstruction. However, the ecological mechanism remains unclear regarding STOP1's regulation of the relationship between rhizosphere PSB and soil P availability.

This study aims to: (i) examine variations in P availability, organic acid, and bacterial community composition between P-rich and P-poor soils, (ii) elucidate the ecological functions of transcription factor STOP1 in regulating organic acid production and P availability, and (iii) identify differences in landscape patterns and functional potentials of rhizosphere bacteria between the YCO3-3 wild type (WT) and *GmSTOP1-3* overexpression (OX) plants. Based on evidence that transcription factor STOP1 supports plant root adaptation to P deficiency (Li and Tian 2023; Liu *et al.* 2025), we hypothesized that *GmSTOP1-3*-mediated oxalate and citrate exudation could enhance soil P availability by recruiting beneficial bacteria for organic-P mineralization in acid soils. Our results emphasize the significance of *GmSTOP1-3*-mediated organic acid exudation in recruiting beneficial bacteria for organic-P mineralization in acid soils.

2. Materials and methods

2.1. Plant materials and experimental design

A field trial utilizing soybean genotype YC03-3 was conducted at Ningxi Experimental Station of South China Agricultural University (23°24′N, 113°64′E), Guangdong Province, China as previously described (Chen *et al.* 2024). The soil properties are detailed in Appendix A. Two P-fertilizer treatments comprising 1,200 kg ha^{-1} (+P) and 600 kg ha^{-1} (–P) triple superphosphate (P) were administered with constant N (300 kg ha^{-1} urea) and K (300 kg ha^{-1} potassium chloride). During the flowering stage, plants were harvested for dry weight and P concentration determination, and roots were collected for qRT-PCR analysis. Simultaneously, rhizosphere soils were analyzed to determine organic acid concentration, P fractions and 16S rRNA gene amplicon sequencing.

For the pot experiment, soils were collected from the previously mentioned field plots receiving +P treatments. After air-drying and sieving (<5 mm), each pot was filled with 1.7 kg of prepared soil. All pots received uniform applications of urea (0.24 g kg^{-1} soil), triple superphosphate (2 g kg^{-1} soil), and KCl (0.4 g kg^{-1} soil) as basal fertilizers. Soybean seeds of WT and OX were directly sown in the prepared soils moistened with deionized water. Following seed germination, transgenic plants underwent confirmation through herbicide resistance analysis and qRT-PCR. Three uniform plants were maintained per pot. At the flowering stage, plants were harvested to determine dry weight and P concentration, and the roots were collected for qRT-PCR analysis. The

rhizosphere soils were analyzed as described below to determine organic acid concentration, phosphatase activity, P fractions and 16S rRNA gene amplicon sequencing. The pot experiment was conducted in a greenhouse at South China Agricultural University, Guangzhou, China.

2.2. Plant and soil sampling

For biomass and plant P content measurement, soybean shoots and roots were oven-dried at 75°C and weighted to determine the biomass. The samples were then ground into powders, digested with H_2SO_4-H_2O_2 reagent, and P concentration was determined using a continuous flow analyzer (Series SA1100, SKALAR, Breda, The Netherlands) as previously described (Chen Q Q *et al.* 2019). The plant P content was calculated by multiplying the plant P concentration by the plant biomass.

The rhizosphere soils were collected according to previously described methods (Wang *et al.* 2021; Chen *et al.* 2024). In brief, root systems with adhering soil were gently shaken in 100 mL of 0.2 mmol L^{-1} $CaCl_2$ solution to dislodge rhizosphere soil. A 25 mL soil suspension subsample was used for determination of phosphatase activity and organic acid. Another 40 mL soil suspension subsample was used for 16S rRNA gene amplicon sequencing. The remaining soil suspension was air-dried and sieved for analysis of soil Pi fractionation.

2.3. Soil chemical properties analyses

Soil pH was measured using a water to soil ratio of 2.5:1 (Chen *et al.* 2024). The Walkley-Black method was employed to measure soil organic carbon (C) (Walkley and Black 1934). Soil total nitrogen (N) concentration was analyzed using the Kjeldahl-distillation titration method (Bremner and Mulvaney 1982). The soil total P was digested with H_2SO_4 and $HClO_4$, and the soil available P was extracted with NH_4F and HCl, after which the concentration of P in each supernatant was determined using the molybdenum blue method at 880 nm (Kuo 1996; Sims 2000). Soil organic P was determined following the method described by Chen *et al.* (2024).

The soil Pi fractionation sequential extraction procedure was performed according to Chen *et al.* (2022), based on the method originally developed by Chang and Jackson (1957). The soil Pi fractions were analyzed through sequential extraction of 1 g of dried soil (0.15 mm) with 1 mol L^{-1} NH_4Cl (Sol-P), 0.5 mol L^{-1} NH_4F (pH 8.2, Al-P), 0.1 mol L^{-1} NaOH (Fe-P), 0.25 mol L^{-1} H_2SO_4 (Ca-P). Concentrations of inorganic P in these extracts were measured using the molybdenum blue colorimetric method of Kuo (1996), using a microplate reader (Thermo Fisher Scientific, USA). The soil total P was determined as described above. The concentration of total organic P was calculated as the difference between the total P and all inorganic P in these extracts.

2.4. Analysis of phosphatase activity

Soil phosphatase activity was measured according to previously established methods (Neumann 2006; Chen *et al.* 2024). In brief, soil suspensions were incubated for 15 min in Na-Ac buffer (200 mmol L^{-1}, pH 5.2) and sodium bicarbonate buffer (200 mmol L^{-1}, pH 8.5) containing 20 mmol L^{-1} ρ-NPP at 30°C to determine acid and alkaline phosphatase (AcP and AlP) activities, respectively. The reaction was terminated by adding 0.5 mol L^{-1} NaOH, and the absorbance was measured at 405 nm using a microplate reader (Thermo Fisher Scientific, USA). Concurrent control samples were analyzed with NaOH added prior to incubation. The soil phosphatase activity was calculated based on the soil pellet dry weight and expressed as the amount of ρ-nitrophenol (NP) released per gram of soil per hour.

2.5. Analysis of organic acid

Organic acid analysis was conducted following previously described methods with minor modifications (Shen *et al.* 2003). Approximately 20 mL of soil suspensions were centrifuged at 3,381×g for 5 min. The supernatants were filtered through a 0.45 μm filter and freeze-evaporated using a freeze-drying vacuum system (Labconco, Kansas, MO, USA). The resulting products were redissolved in 1 mL deionized H_2O and analyzed using high-performance liquid chromatography (HPLC, Agilent 1260 Infinity LC System, Agilent Technologies, USA) after passing through a 0.22 μm filter. HPLC quantitative determination was performed on an Agilent Polaris C18-A column (4.6 mm×250 mm, 3 μm). The mobile phase consisted of 0.1% metaphosphate with a flow rate of 0.7 mL min^{-1} and injection volume of 20 μL at 40°C column temperature. Organic acids (citrate and oxalate) were detected using a diode array detector at 210 nm and quantified by comparing retention time and absorption spectra with standard curves.

2.6. RNA extraction and qRT-PCR analysis

RNA extraction and qRT-PCR analysis were performed according to previously described methods (Zhu *et al.* 2024). Total RNA from soybean roots was extracted using TRIzol Reagent (OMEGA Bio-Tek, Norcross, GA, USA) and treated with RNase-free DNase I (Invitrogen, Carlsbad, CA, USA). Approximately 1 μg of total RNA was reverse-transcribed using a reverse transcription kit (Promega, Madison, WI, USA) to synthesize first-strand cDNA following manufacturer protocols. The qRT-PCR analysis was performed using SYBR Green PCR master mix (Promega, USA) on an ABI7500 real-time PCR system (Thermo Fisher Scientific, Waltham, MA, USA). Expression levels of genes including *GmMATE2/13* and oxalate transporter (*GmOT1/2*) were analyzed. *GmMATE2* and *GmMATE13* function as citrate transporter genes in soybean, enhancing citrate secretion and Al tolerance/Pi starvation responses (Gao *et al.* 2024; Liu *et al.* 2025). The *AtOT* in Arabidopsis (*A. thaliana*) and *HbOT1/2* in rubber tree (*Hevea brasiliensis*) were characterized as oxalate transporters (Yang *et al.* 2022, 2023). The housekeeping gene *GmEF-1a* (*Glyma.17G186600*) served as an internal control, and relative expression levels were calculated as the ratio of target gene transcripts to housekeeping gene transcripts. Primers used for qRT-PCR analysis are listed in Appendix B.

2.7. High-throughput sequencing and bioinformatics analysis

Rhizosphere soil DNA was extracted from 0.25 g of fresh

soil per sample using the TGuide S96 Magnetic Soil/Stool DNA Kit (Tiangen Biotech, Co., Ltd., Beijing, China) following the manufacturer's protocol. DNA quality and concentration were assessed through agarose gel electrophoresis and a NanoDrop ND-2000 spectrophotometer (Thermo Fisher Scientific, USA), respectively. The full-length bacterial 16S rRNA gene sequences were amplified from high-quality DNA samples using universal primers 27F (5′-AGRGTTYGATYMTGGCTCAG-3′) and 1492R (5′-TASGGHTACCTTGTTASGACTT-3′). Subsequently, SMRTbell libraries were constructed from purified, quantified, and homogenized PCR products, and 16S rRNA gene sequencing was performed using single molecule real-time sequencing (SMRT) on the PacBio platform (Pacific Biosciences, Menlo Park, CA, USA). All raw 16S rRNA gene sequencing data from both field experiment and pot trial have been deposited in the NCBI Sequence Read Archive (SRA) database under accession numbers PRJNA1135447 and PRJNA1135449, respectively.

The circular consensus sequences (CCS) reads were generated by correcting raw reads using SMRT Link (v. 8.0), followed by barcode identification, length filtering, and chimera removal using lima (v. 1.7.0) and UCHIME algorithm (v. 8.1) to obtain effective CCS reads. These effective CCS reads were clustered into operational taxonomic unit (OTU) at 97% similarity thresholds using USEARCH (v.10.0). Taxonomic annotation of each OTU representative sequence was conducted using the SILVA bacterial 16S rRNA gene database (Release132, http://www.arb-silva.de) with the RDP Classifier tool (v. 2.2) at a confidence cutoff of 0.8. The detected communities were subsequently identified and annotated at various taxonomic levels (e.g., phylum and order).

QIIME2 software was utilized to analyze rarefaction curves and alpha diversity indices (ACE, Chao1, Simpson, Shannon). Beta diversity analysis, comprising principal coordinate analysis (PCoA) and permutational multivariate analysis of variance (PERMANOVA), was performed using QIIME and R software. Redundancy analysis (RDA) evaluated the relationships between soil bacterial community composition and rhizosphere oxalate and citrate concentrations. Metastats analysis was conducted at the order and genus level to identify differentially abundant taxa between groups (Nizigiyimana *et al.* 2022). The functional genes involved in P-cycling of bacterial communities in soybean rhizosphere soil were predicted using Phylogenetic Investigation of Communities by Reconstruction of Unobserved States (PICRUSt2) and the KEGG database (https://www.kegg.jp/) (Douglas *et al.* 2020; Li *et al.* 2022). The KO numbers, gene names, functions, and classifications of P cycling-associated genes are presented in Appendix C. All analyses were performed by Biomarker Technologies Corporation (Beijing, China) and the BMK Cloud Platform (www.biocloud.net).

2.8. Statistical analysis

Statistical analyses and standard error calculations were performed using Microsoft Excel 2019 (Microsoft Company, United States). The Student's *t*-test was conducted using the SPSS program (v. 21.0; SPSS Institute, United States). Data visualization included radar charts generated by OriginPro 2024b and Pearson correlation heatmaps created using OmicStudio tools at https://www.omicstudio.cn/tool. Phylogenetic analysis of soybean oxalate transporter (OT) genes was conducted using MEGA-X with the neighbor-joining method and 1,000 bootstrap replicates. A Venn diagram illustrated the unique and shared differentially abundant bacterial orders among the groups. The Mantel test and Spearman correlation heatmaps examined relationships between differentially bacterial orders, plant functional variables, and soil P-cycling genes. Co-occurrence networks were generated using the tutu cloud platform to analyze relationships between bacterial OTUs with average relative abundance exceeding 0.04%. Spearman coefficients between OTUs were calculated, including correlations with $r>0.8$ and $P<0.05$ in the network. Network visualization was performed using Gephi 0.9.2 software. Spearman correlation networks were created using the metware cloud platform to evaluate relationships between differentially bacterial orders, bacterial P-cycling genes, and soil properties with $r>0.8$ and $P<0.05$.

3. Results

3.1. Effects of P fertilization on soybean growth and P fractions in rhizosphere soil

Field experiments were conducted to examine the relationships among soybean plant growth, root organic acid exudates, and rhizosphere bacterial community in response to Pi availability. Sufficient P-fertilizer application led to elevated soil pH and higher concentrations of organic carbon, total N, total P, available Pi, and organic P in soils (Appendix A). Sufficient P also enhanced plant dry weight and P content (Fig. 1-A–C). Conversely, soybean rhizosphere oxalate and citrate concentrations increased under –P treatment (Fig. 1-D and E). Notably, the rhizosphere oxalate concentration in –P treatment was approximately 4-fold higher than in the +P treatment (Fig. 1-D). Furthermore, P-fertilizer significantly affected rhizosphere P fractions. The concentrations of rhizosphere iron bound P (Fe-P), organic P, and total P in –P treatment were 64, 70, and 47% lower than those in the +P treatment, respectively (Fig. 1-F–H). However, aluminum bound P (Al-P) and calcium bound P (Ca-P) concentrations remained similar between +P and –P treatments (Fig. 1-I and J). Pearson correlation analysis revealed that oxalate concentration exhibited significant negative correlations with rhizosphere Fe-P ($P=0.049$) and organic P concentrations ($P=0.037$) (Fig. 1-K).

3.2. Effects of P fertilization on the diversity and composition of soybean rhizosphere bacterial community

The rhizosphere bacterial communities were analyzed through 16S rRNA gene amplicon sequencing, yielding an average of 12,686 effective CCS reads per sample (Appendix D). The rarefaction curves approached saturation plateaus, indicating sufficient sequencing depths across all samples for diversity analysis (Appendix E). The +P treatment significantly enhanced the α-diversity of the soybean rhizosphere bacterial community, as evidenced by higher

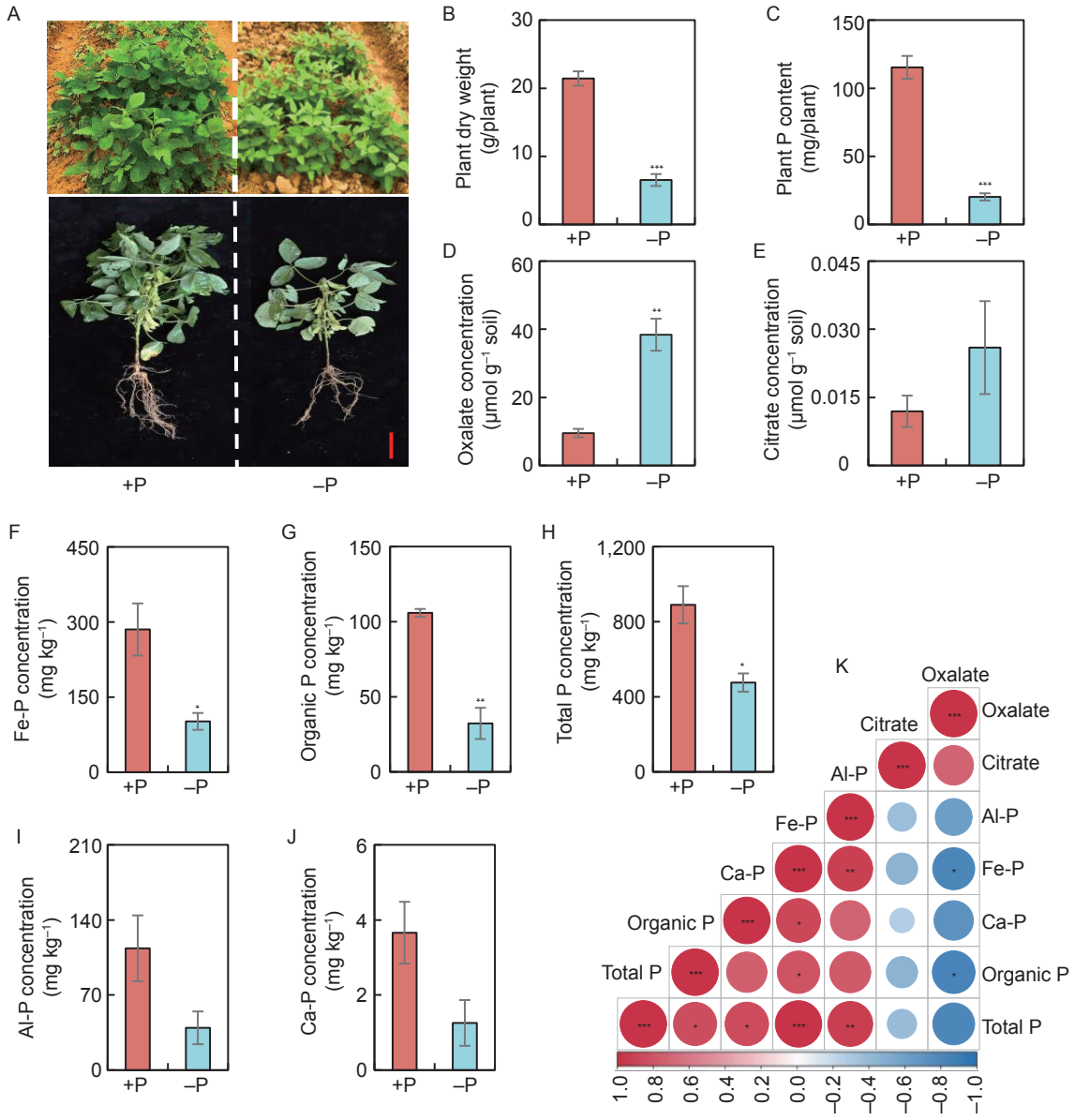


Fig. 1 Impact of phosphorus (P) fertilization on soybean development and P fractions in rhizosphere soil. A, plant phenotype, Bar=10 cm. B, plant dry weight. C, plant phosphorus content. D and E, rhizosphere oxalate (D) and citrate (E) concentrations. F–J, concentrations of iron bound P (Fe-P) (F), organic P (G), total P (H), aluminum bound P(Al-P) (I) and calcium bound P (Ca-P) (J). The data presented are means of three replicates with standard error (n=3). Asterisks denote significant differences between 1,200 kg ha^{-1} (+P) and 600 kg ha^{-1} (–P) treatments determined by Student's t-test (*, P<0.05, **, P<0.01, ***, P<0.001). K, correlation between rhizosphere organic acid concentration and P fractions. The heatmap colors represent correlation coefficients (r values), with the legend below showing the color range of different r values. Red indicates positive correlation, blue indicates negative correlation. Asterisk denotes statistically significant correlation (*, P<0.05, **, P<0.01, ***, P<0.001).

ACE and Chao1 indexes (Fig. 2-A). PCoA demonstrated that bacteria in +P and –P treatments formed two distinct clusters, separating along the first coordinate axis (PERMANOVA, R^2=0.367, P=0.001) (Fig. 2-B). RDA indicated that bacterial community composition changes correlated with rhizosphere oxalate (R^2=0.965, P=0.001) and citrate (R^2=0.913, P=0.014) concentration (Fig. 2-C; Appendix F). At the phylum level, Proteobacteria demonstrated the highest relative abundance, followed by Bacteroidota, Acidobacteriota, Chloroflexi, Patescibacteria, Actinobacteriota, Verrucomicrobiota, Planctomycetota, and Firmicutes (Fig. 2-D). The –P treatments exhibited higher relative abundances of Acidobacteriota and Chloroflexi but lower relative abundances of Bacteroidota and Patescibacteria compared to +P treatments (Fig. 2-D).

3.3. Relationships between bacterial orders and soil environmental factors

Metastats analysis identified differentially abundant taxa at the order level between +P and –P treatments. The analysis revealed significant enrichments of unclassified_ Thermodesulfovibrionia, Vicinamibacterales, Tepidisphaerales,

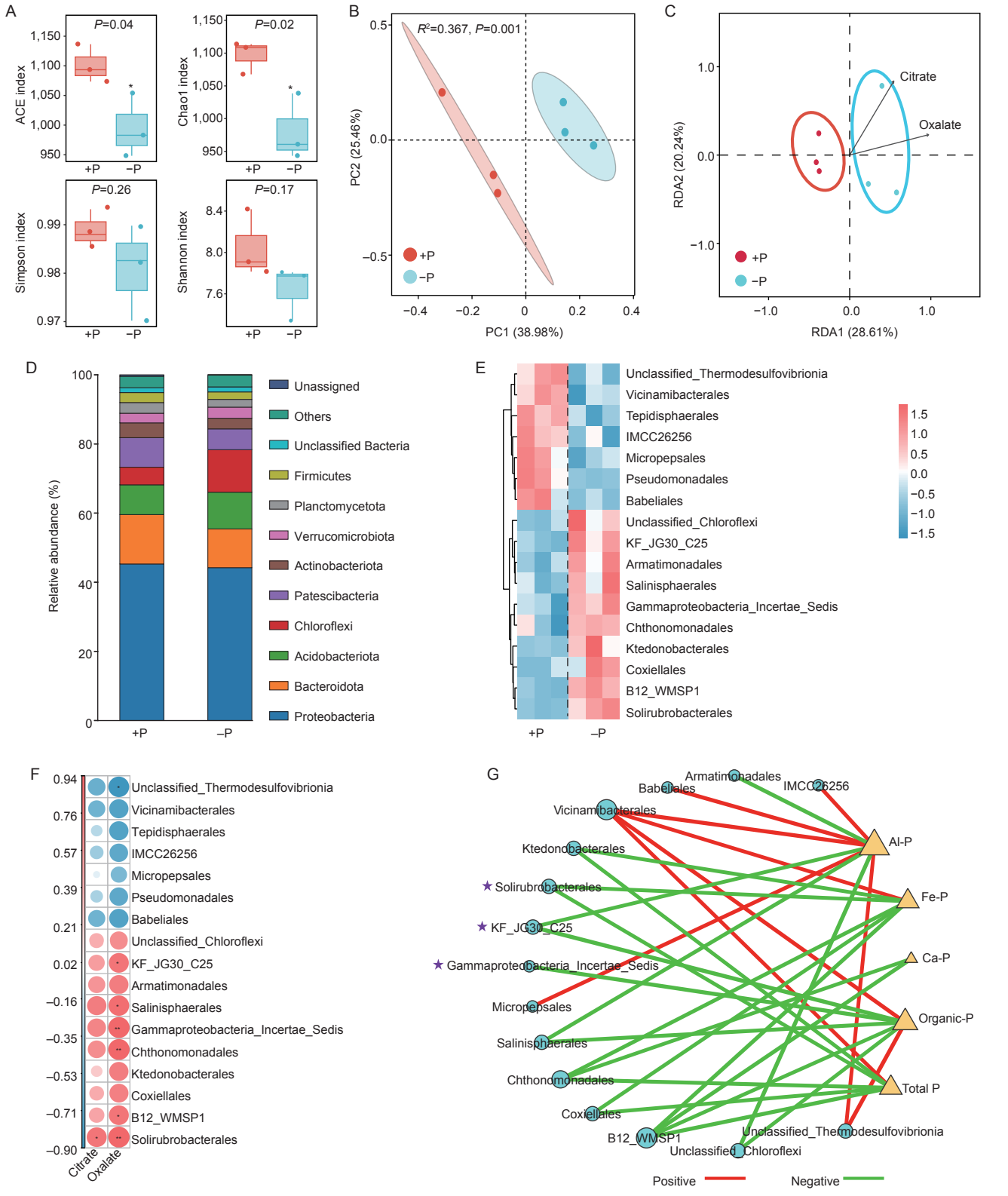


Fig. 2 Effects of P fertilization on the diversity and composition of soybean rhizosphere bacterial communities. A, alpha-diversity of the bacterial community. Asterisks indicate significant differences between 1,200 kg ha^{-1} (+P) and 600 kg ha^{-1} (–P) treatments according to Student's *t*-test (*, $P<0.05$). B, principal coordinate analysis (PCoA) ordinations of bacterial communities in the soybean rhizosphere at operational taxonomic unit level. C, redundancy analysis (RDA) examining the relationships between bacterial community composition at the order level and rhizosphere oxalate and citrate concentrations. D, relative abundances of bacterial communities at the phylum level in the 1,200 kg ha^{-1} (+P) and 600 kg ha^{-1} (–P) treatments. E, heatmap showing differentially abundant taxa at the order level between +P and –P treatments. The abundance data were transformed using Z-scores. F, heatmaps of Spearman correlation analysis between bacterial orders and rhizosphere oxalate and citrate concentrations. Asterisk indicates statistically significant correlation (*, $P<0.05$, **, $P<0.01$). G, network constructed through correlation of bacterial orders (blue nodes) and rhizosphere P fractions (yellow triangles). Al-P, aluminum bound P; Fe-P, iron bound P; Ca-P, calcium bound P. Node size corresponds to the degree of each node.

IMCC26256, Micropepsales, Pseudomonadales, and Babeliales in the +P treatment, while unclassified_Chloroflexi, KF−JG30−C25, Armatimonadales, Salinisphaerales, Gammaproteobacteria_Incertae_Sedis, Chthonomonadales, Ktedonobacterales, Coxiellales, B12−WMSP1, and Solirubrobacterales showed significant enrichment in the –P treatment (Fig. 2-E; Appendix G).

In the –P treatment, most bacterial orders showed significant positive correlations with rhizosphere oxalate concentration (P<0.05), except for unclassified_Chloroflexi, Armatimonadales, Ktedonobacterales, and Coxiellales. Additionally, Solirubrobacterales demonstrated a significant positive correlation with rhizosphere citrate concentration (P<0.05) (Fig. 2-F). The relative abundances of unclassified_Chloroflexi, KF−JG30−C25, and Salinisphaerales exhibited significant negative correlations with rhizosphere Al-P and organic-P concentrations (P<0.05), while Gammaproteobacteria_Incertae_Sedis showed a significant negative correlation with rhizosphere organic-P concentration (P<0.01) (Fig. 2-G). The relative abundances of Chthonomonadales, Ktedonobacterales, Coxiellales, B12−WMSP1, and Solirubrobacterales displayed significant negative correlations with rhizosphere Fe-P and total P concentrations (P<0.05) (Fig. 2-G). At the genus level, *Acidibacter* (from Gammaproteobacteria_Incertae_Sedis) and *Conexibacter* (from Solirubrobacterales) showed significant enrichment in the –P treatment. Both genera demonstrated significant positive correlations with rhizosphere oxalate concentration while showing significant negative correlations with rhizosphere organic-P and Fe-P concentrations, respectively (P<0.05) (Appendix H). These findings suggest that soybean may recruit specific rhizobacteria for P-forage in P-deficient acid soils through enhanced oxalate and citrate exudation.

3.4. Effects of *GmSTOP1-3* overexpression on soybean growth and rhizosphere soil properties

Previous research has demonstrated that *GmSTOP1-3* regulates soybean root organic acid exudation by controlling the expression of genes involved in organic acid metabolism and secretion (Liu *et al.* 2025). qRT-PCR analysis revealed significantly elevated expression levels of four target genes, including *GmMATE2/13* and *GmOT1/2*, in the OX compared to WT (Fig. 3-A and B). Of these genes, *GmMATE2* and *GmMATE13* were associated with citrate exudation (Liu *et al.* 2025), while GmOT1 and GmOT2 exhibited high similarity with oxalate transporter in AtOT, brown rot fungus (*Fomitopsis palustris*) (FpOAR), rubber tree (*H. brasiliensis*) (HbOT1 and HbOT2) (Appendix I). Furthermore, all these genes showed upregulation under low P conditions (Appendix J).

Pot culture experiments were conducted to investigate the effects of exudated organic acids on microbiota in OX and WT (Fig. 3-C). The results demonstrated that compared to WT, *GmSTOP1-3* overexpression significantly enhanced root citrate and oxalate exudation, with 3.4 and 2.7 folds higher concentrations in OX rhizosphere, respectively (Fig. 3-D and E). Additionally, OX plants exhibited increased plant dry weight, plant P content, and rhizosphere AcP and AlP activities (Fig. 3-F; Appendix K-a–d). The rhizosphere P fractions were substantially affected by *GmSTOP1-3* overexpression. The rhizosphere Al-P, Fe-P, organic P, and total P concentrations in OX were 13, 7, 11, and 10% lower than WT, respectively (Fig. 3-F; Appendix K-e–h). While Sol-P was 35% higher and Ca-P was 8% lower in OX compared to WT, these differences were not statistically significant (P=0.54 in Sol-P and P=0.47 in Ca-P) (Fig. 3-F; Appendix K-i–j). Pearson correlation analysis showed that the oxalate and citrate concentrations were significantly positively correlated with plant dry weight (P=0.033 and 0.007, respectively), plant P content (P=0.013 and 0.044, respectively), and AcP activity (P=0.011 and 0.0005, respectively). Conversely, significant negative correlations were observed with rhizosphere Al-P (P=0.014 and 0.0007, respectively), Fe-P (P=0.033 and 0.0001, respectively), organic P (P=0.028 and 0.005, respectively), and total P (P=0.029 and 0.0002, respectively) concentrations (Fig. 3-G). These findings suggest that *GmSTOP1-3*-mediated organic acid exudation may participate in soil P remobilization.

3.5. Effects of *GmSTOP1-3* overexpression on diversity and composition of soybean rhizosphere bacterial communities

The 16S rRNA gene amplicon sequencing yielded an average of 12,545 effective CCS reads per sample, with rarefaction curves showing gradual saturation (Appendices L and M). The bacterial Simpson and Shannon indices were significantly higher in OX compared to WT (P<0.05) (Fig. 4-A). PCoA revealed clear separation between OX and WT bacterial communities (PERMANOVA, R^2=0.605, P=0.001), with PC1 accounting for 72.8% and PC2 explaining 18.31% of the variance (Fig. 4-B). RDA indicated that bacterial community composition changes correlated with rhizosphere oxalate (R^2=0.827, P=0.019) and citrate (R^2=0.918, P=0.025) concentration (Fig. 4-C; Appendix N).

Proteobacteria demonstrated the highest relative abundance at the phylum level. Among the top ten dominant phyla, OX exhibited higher relative abundances of Chloroflexi, Acidobacteriota, Patescibacteria, and Firmicutes compared to WT (Fig. 4-D). At the order level, Burkholderiale showed the highest relative abundance across all samples. *GmSTOP1-3* overexpression resulted in increased relative abundances of Xanthomonadales, Chitinophagales, Ktedonobacterales, unclassified_Alphaproteobacteria, Saccharimonadales, and Acidobacteriales compared to WT (Fig. 4-E).

Analysis of microbial co-occurrence networks revealed that OX plants exhibited more complex and robust networks than WT, as evidenced by higher numbers of edges, correlations, average degree and weighted degree, and graph density (Fig. 4-F; Appendix O).

3.6. Linkages among bacterial orders and soil environmental factors

Metastats analysis at the order level identified distinct bacterial taxa between OX and WT (Fig. 5-A; Appendix P). The analysis revealed significant enrichment of Gammaproteobacteria_Incertae_Sedis, KF_JG30_C25, and

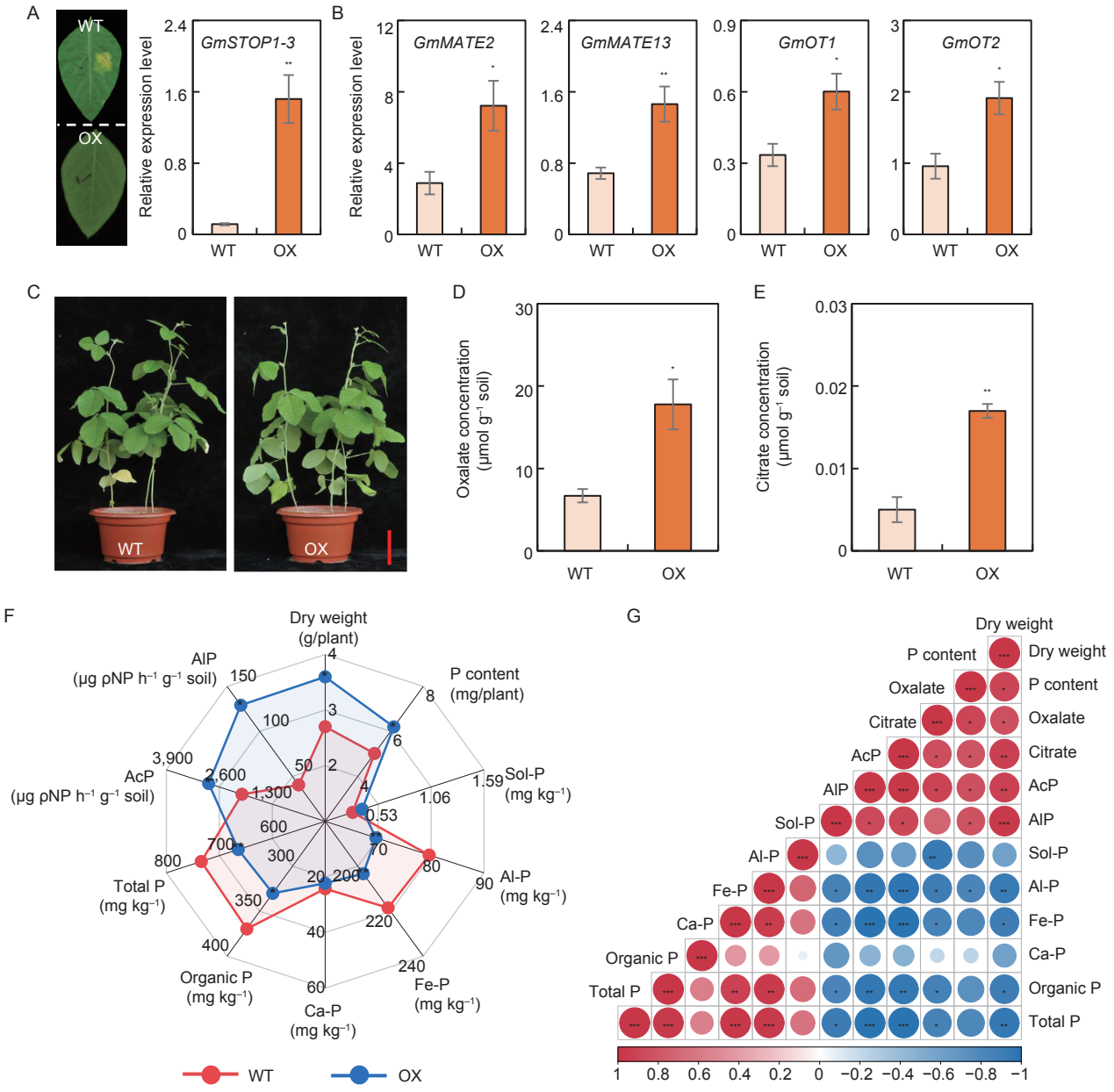


Fig. 3 Effects of *GmSTOP1-3* overexpression on soybean growth and rhizosphere soil properties. A, herbicide tolerance assessment and qRT-PCR analysis in wild type (WT) and transgenic line confirming *GmSTOP1-3* overexpression (OX). B, expression level of *GmMATE2/13* and *GmOT1/2* in roots of WT and OX. C, plant phenotype. Bar=10 cm. D and E, rhizosphere oxalate (D) and citrate (E) concentrations. F, soybean growth, rhizosphere organic acid concentration, phosphatase activity and P fractions. Data presented are means of three or more replicates with standard error (n≥3). Asterisks denote significant differences between WT and OX determined by Student's t-test (*, P<0.05, **, P<0.01). G, correlation analysis of soybean growth, rhizosphere organic acid concentration, phosphatase activity and P fractions. AcP, acid phosphatase activity; AlP, alkaline phosphatase activity; Sol-P, easily soluble P; Al-P, aluminum bound P; Fe-P, iron bound P; Ca-P, calcium bound P. Asterisks indicate statistically significant correlation (*, P<0.05, **, P<0.01, ***, P<0.001).

Solirubrobacterales in OX, which were similarly enriched in the WT rhizosphere under P-deficient conditions (Fig. 5-A and B). Spearman correlation analysis indicated that the relative abundances of these three bacterial orders exhibited significant positive correlations with rhizosphere oxalate and citrate concentrations (P<0.05) (Fig. 5-C). These findings suggest that Gammaproteobacteria_Incertae_Sedis, KF_JG30_C25, and Solirubrobacterales were attracted by soybean root-exuded citrate and oxalate.

Additional Spearman correlation analysis revealed that KF_JG30_C25, Solirubrobacterales, and Gammaproteobacteria_Incertae_Sedis demonstrated significant positive correlations with both AcP and AlP activities (Fig. 5-D). The relative abundances of KF_JG30_C25 and Solirubrobacterales showed significant positive correlations with plant biomass and P content, while exhibiting negative correlations with rhizosphere Al-P, Fe-P, organic-P, and total P concentrations (P<0.05) (Fig. 5-D). Additionally, Gammaproteobacteria_Incertae_Sedis displayed significant positive correlation with plant biomass and negative correlation with Fe-P, Ca-

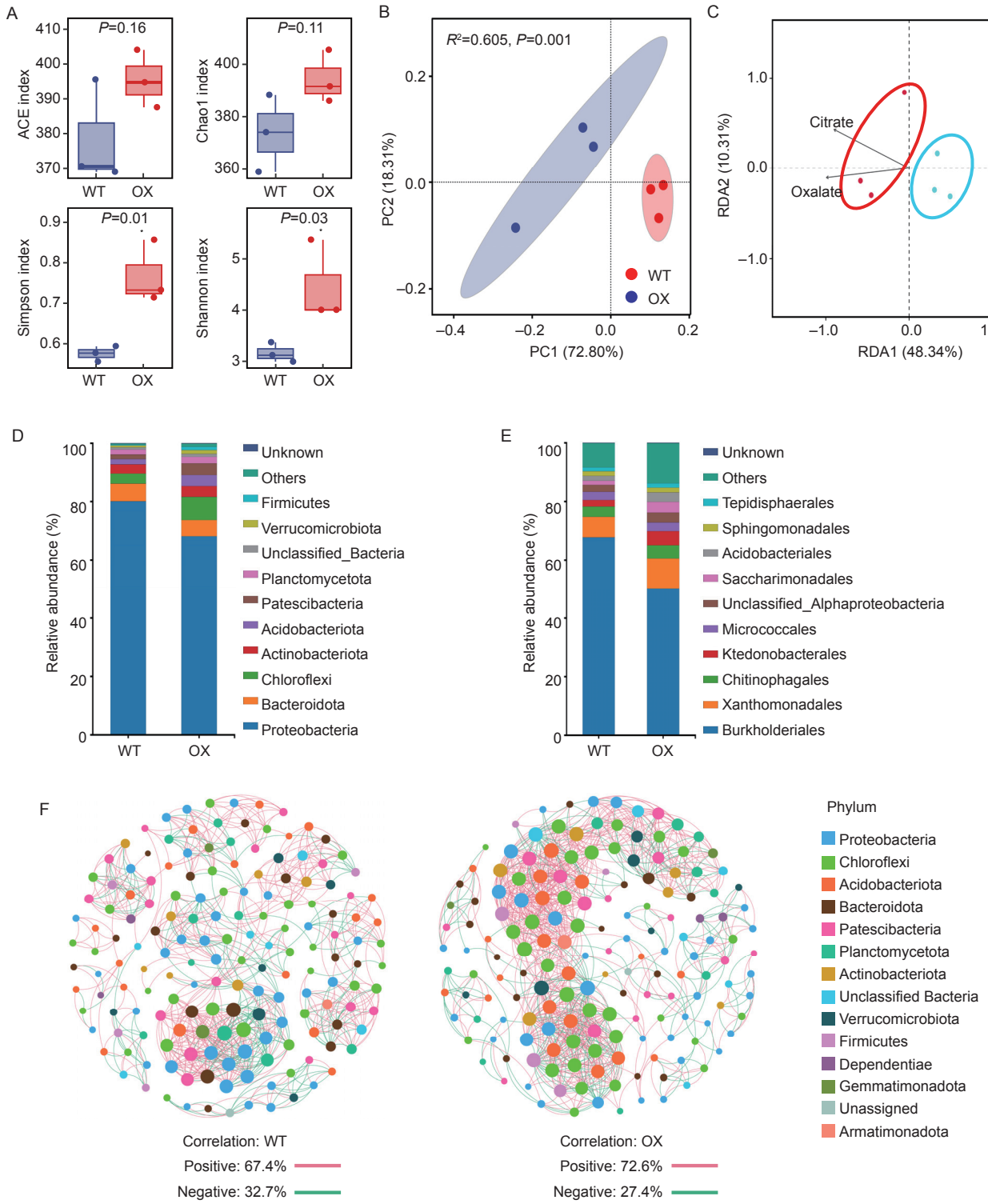


Fig. 4 Effects of *GmSTOP1-3* overexpression on diversity and composition of soybean rhizosphere bacterial communities. A, alpha-diversity. Asterisks indicate significant differences between wild type (WT) and *GmSTOP1-3* overexpression (OX) plants based on the Student's *t*-test (*, $P<0.05$). B, principal coordinate analysis (PCoA) ordinations of bacterial communities in the soybean rhizosphere at OTU level. C, redundancy analysis (RDA) examining the relationships between bacterial community composition at the order level and rhizosphere oxalate and citrate concentrations. D and E, relative abundances of the bacterial community at the phylum level (D) and order level (E). F, co-occurrence network of the rhizosphere bacterial community for WT and OX. Nodes are colored according to bacterial phylum. Node size represents the degree of connection. Edge color indicates positive (red) and negative (green) correlations.

P, and total P concentrations ($P<0.05$) (Fig. 5-D). At the genus level, the relative abundances of *Acidibacter* (from Gammaproteobacteria_Incertae_Sedis) and *Conexibacter* (from Solirubrobacterales) showed significant positive correlation with rhizosphere oxalate concentration and negative correlation with rhizosphere Al-P, Fe-P, organic-P,

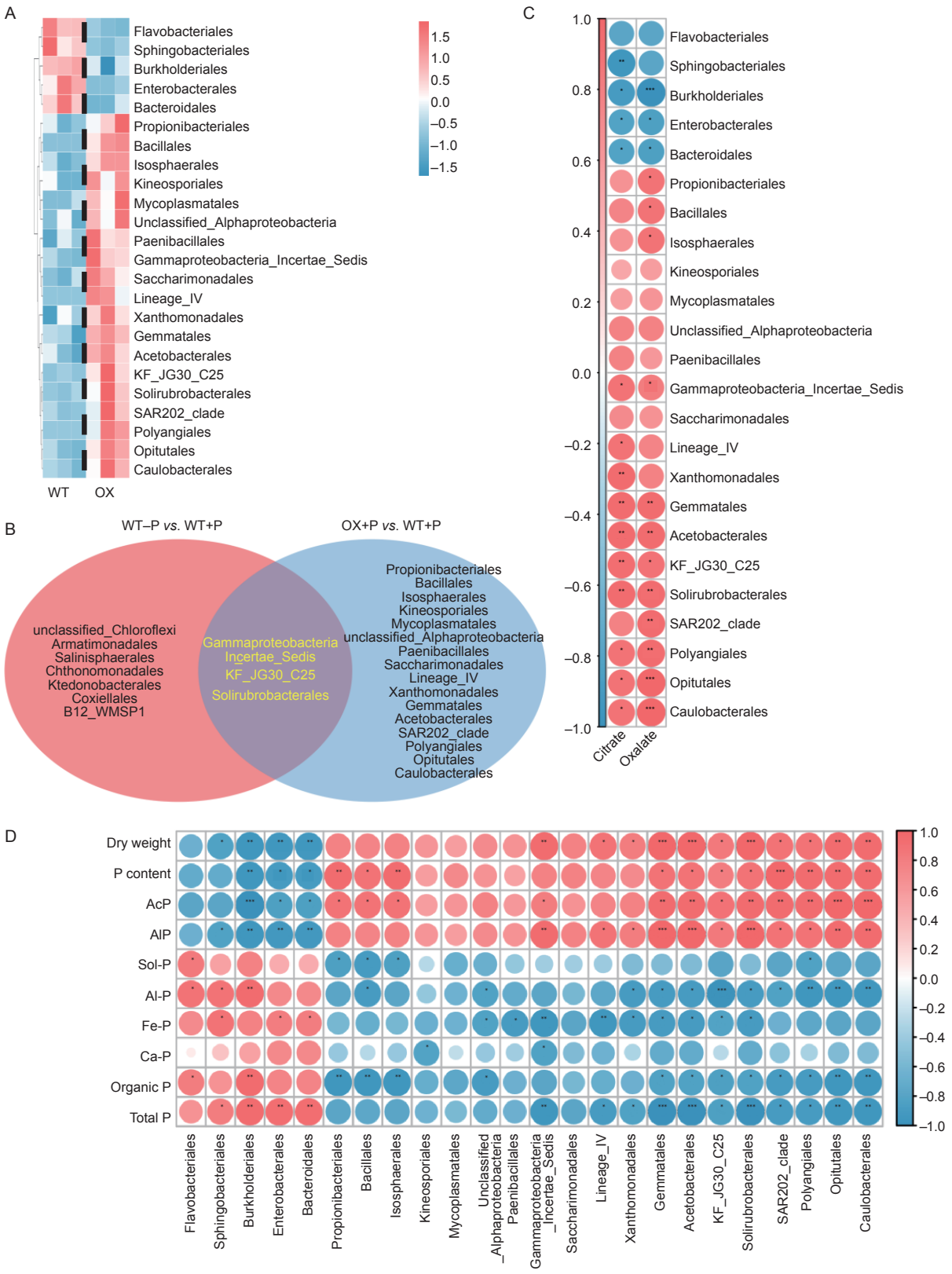


Fig. 5 Associations between bacterial orders and soil environmental parameters. A, heatmap depicting differentially abundant taxa at the order level between wild type (WT) and *GmSTOP1-3* overexpression (OX) plants. The abundance data were normalized using Z-scores. B, Venn diagram illustrating bacterial orders that are unique and shared between WT–P treatment *vs.* WT+P treatment and OX *vs.* WT. C, heatmaps of the Spearman correlation analysis between the differentially abundant bacterial orders and rhizosphere oxalate and citrate concentrations. D, heatmaps of the Spearman correlation analysis between the differentially abundant bacterial orders and soybean growth, rhizosphere phosphatase activity and P fractions. AcP, acid phosphatase activity; AlP, alkaline phosphatase activity; Sol-P, easily soluble P; Al-P, aluminum bound P; Fe-P, iron bound P; Ca-P, calcium bound P. Asterisks indicate statistically significant correlation (*, $P<0.05$, **, $P<0.01$, ***, $P<0.001$).

and total-P concentrations (P<0.05) (Appendix Q-a). Furthermore, significant enrichment of *Acidibacter* and *Conexibacter* was observed in OX and the WT rhizosphere under P-deficient conditions (Appendix Q-b). These findings indicate that these species may enhance plant P acquisition through remobilization of sparingly soluble P sources.

3.7. Correlations between bacterial orders, P-cycling genes and environmental factors

To examine the effects of *GmSTOP1-3* overexpression on P cycling-related functional genes in soil bacterial communities, PICRUSt2 analysis was conducted to predict the relative abundance of P cycling genes based on 16S rRNA gene sequencing data (Fig. 6-A). The analysis revealed higher relative abundances in the OX line compared to WT for genes involved in organic P-mineralization (*olpA*, *phoN*, *phoAB*, *phoD* and *appA*), inorganic P-solubilization (*ppk*, *ppx* and *gcd*), P-uptake and transport (*glpP*, *pstBCAS*, and *pitAB*), and Pi-starvation response regulation (*phoB*, *phoR* and *phoU*). Conversely, the relative abundances of *aphA*, *pqqBCDE*, *ugpBAEC* and *pit* were lower in the OX line compared to WT (Fig. 6-A).

Mantel test was employed to identify relationships between bacterial orders, P-cycling genes and environmental factors**.** The analysis demonstrated significant relationships between oxalate, citrate, AcP, AlP, Al-P, Fe-P, organic P, and total P with the abundances of genes coding for organic P-mineralization and inorganic-P solubilization. Additionally, oxalate, AcP, and AlP showed significant relationships with the abundances of genes coding for P-uptake and transport. Furthermore, oxalate, citrate, AcP, AlP, and Fe-P demonstrated significant relationships with the abundances of genes coding for P-starvation response (Fig. 6-B; Appendix R).

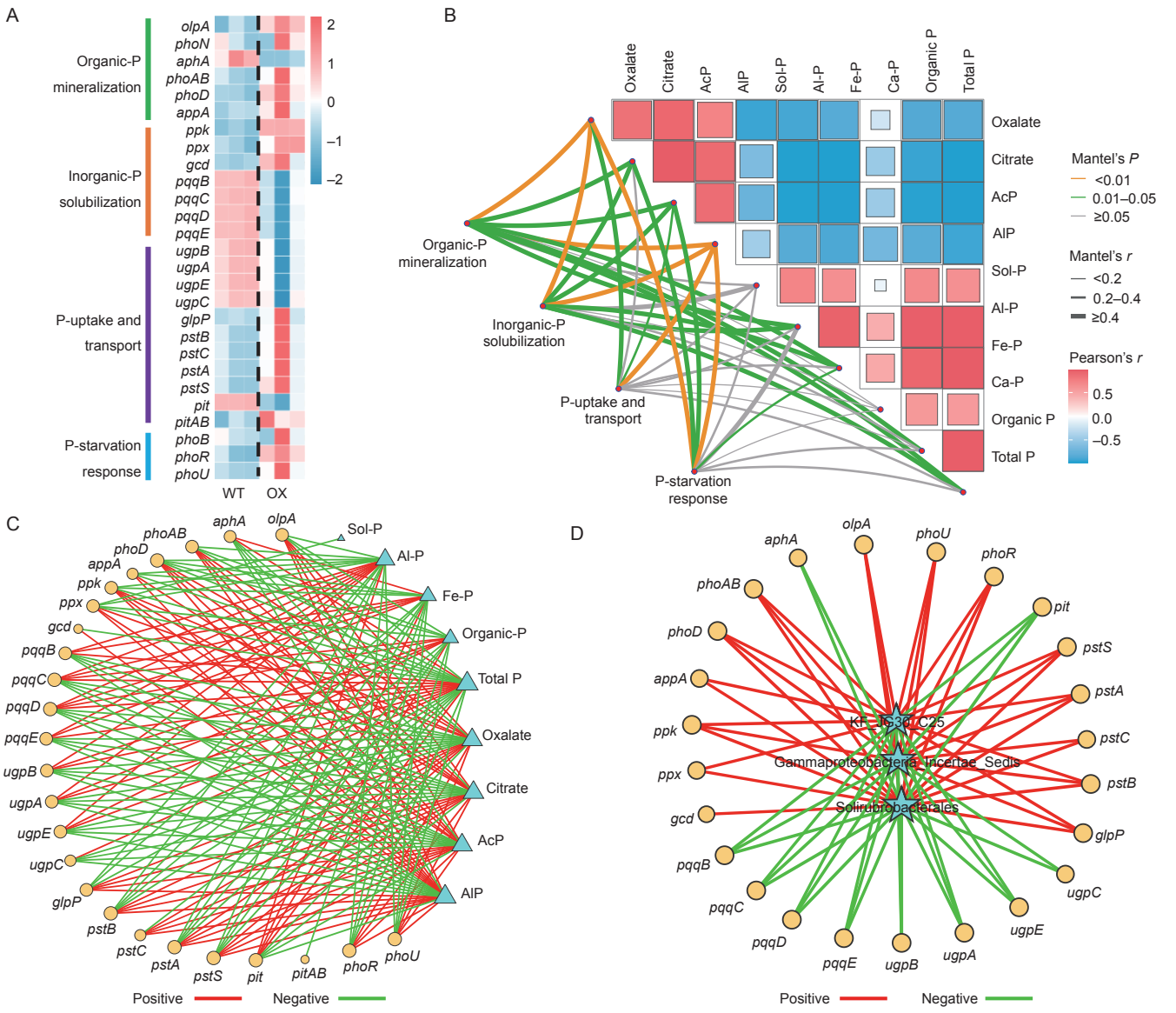
Spearman correlation analysis was conducted to investigate the relationships between soil P-cycle genes and both environmental factors and bacterial orders. The correlation heatmap revealed that the relative abundances of genes involved in organic P-mineralization (*olpA*, *phoAB* and *phoD*), inorganic P-solubilization (*ppk* and *ppx*), P-uptake and transport (*glpP* and *pstBCAS*), and P-starvation response (*phoR* and *phoU*) exhibited significant positive correlations with oxalate and citrate concentrations, AcP and AlP activities, while showing negative correlations with Al-P, Fe-P, organic P and total P concentrations (P<0.05) (Fig. 6-C). Furthermore, the relative abundances of three bacterial orders Gammaproteobacteria_Incertae_Sedis, KF_JG30_C25 and Solirubrobacterales, which were enriched in OX rhizosphere, demonstrated significant positive correlations with the relative abundances of *olpA*, *phoAB* and *phoD* (organic P-mineralization), *ppk* (inorganic P-solubilization), *glpP* and *pstBAS* (P-uptake and transport), as well as *phoR* and *phoU* (P-starvation response) (P<0.05) (Fig. 6-D). These findings suggest that the bacteria influenced by *GmSTOP1-3* may participate in P recycling through these P-cycling genes.

4. Discussion

4.1. The P-regulated bacterial community in soybean rhizosphere is related to root organic acid exudation

Plants have developed multiple adaptive strategies to manage P deficiency in acid soils (Liang *et al.* 2014; Mo *et al.* 2022; Li *et al.* 2024; Yang *et al.* 2024). A primary mechanism involves enhanced secretion of root exudates, particularly organic acids and phosphatases, which facilitate insoluble soil P mobilization (Liang *et al.* 2014; Mo *et al.* 2022; Li *et al.* 2024; Yang *et al.* 2024). P-starvation induced organic acid secretion has been documented in numerous plant species (Nwoke *et al.* 2008; Peng *et al.* 2018; Wen *et al.* 2019). Root-exuded organic acids primarily function by directly solubilizing sparingly soluble P resources (Wang *et al.* 2015; Peng *et al.* 2018). When root exudated malate was enhanced through overexpression of genes involved in malate metabolism and transportation, the transgenic cotton (*Gossypium herbaceum*) and Arabidopsis plants demonstrated enhanced utilization of Ca-P, Al-P and Fe-P resources (Wang *et al.* 2015; Peng *et al.* 2018). Consistent with these findings, this study demonstrated that low-P treatment increased citrate and oxalate exudation in soybean genotype YC03-3 (Fig. 1-D and E). Notably, oxalate concentration exhibited a strong negative correlation with rhizosphere Fe-P and organic P concentration (Fig. 1-K). The remobilization of sparingly soluble Fe-P and Al-P resources may be attributed to direct solubilization by root-exuded citrate and oxalate (Nwoke *et al.* 2008). However, direct effects of organic acid on organic P remobilization are not readily explicable. A recent study indicated that soybean rhizosphere organic P recycling primarily depends on acid phosphatase activity derived from specific beneficial bacteria under low P conditions (Chen *et al.* 2024). Therefore, root exuded organic acid may enhance organic P remobilization by attracting beneficial phosphate-solubilizing microorganism communities.

The diversity and structure of plant rhizosphere bacterial communities are significantly influenced by P availability (Chen X D *et al.* 2019; Tian *et al.* 2020; Liu *et al.* 2023; Chen *et al.* 2024). For instance, compared to the P90 treatment, the P0 treatment enhanced the relative abundance of Bacillales and Pseudomonadales, which were identified as primary taxa affecting P dynamics (Tian *et al.* 2020). In alignment with these findings, our results demonstrated that bacterial community richness and diversity were reduced in the –P soils, with distinct bacterial community separation between +P and –P soils (Fig. 2-A and B). This observation aligns with a recent study examining rhizosphere bacterial communities in six soybean genotypes, which reported decreased bacterial community richness and diversity in low-P soils (Chen *et al.* 2024). Notably, the bacterial community in –P soils showed positive correlation with rhizosphere citrate and oxalate concentration (Fig. 2-C). To determine which bacterial orders were associated with root-exudated citrate and oxalate, Metastats and Spearman correlation heatmaps analyses revealed that under –P conditions, unclassified_Chloroflexi, KF−JG30−C25, Armatimonadales, Salinisphaerales, Gammaproteobacteria_Incertae_Sedis, Chthonomonadales, Ktedonobacterales, Coxiellales,



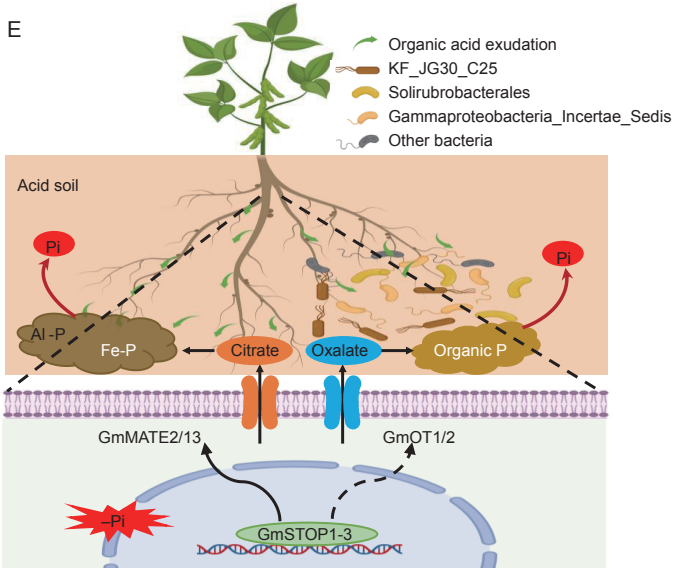


Fig. 6 Correlations between bacterial orders, P-cycling genes, and environmental factors. A, heatmap depicting the relative abundance of soil P-cycling genes predicted by PICRUSt2. The abundance data underwent Z-score transformation. B, mantel test analyzing the relationship between soil environmental factors and the relative abundance of P-cycling genes. C, network analysis illustrating correlations between soil P-cycling genes (yellow nodes) and soil properties (blue triangles). D, network analysis demonstrating correlations between bacterial P-cycling genes (yellow nodes) and the differentially abundant bacterial orders (blue five-pointed star) shared between WT–P treatment *vs.* WT+P treatment and OX *vs.* WT. Node size indicates the degree of each node. E, schematic representation of how soybean *GmSTOP1-3*-mediated organic acid exudation facilitates the recruitment of beneficial bacteria for organic-P mineralization in acid soils. P starvation upregulates *GmSTOP1-3*, which enhances citrate and oxalate exudation by regulating the transcription of organic acid transporter genes, including *GmMATE2/13* and *GmOT1/2*. This enhanced citrate and oxalate exudation recruits and enriches beneficial phosphate-solubilizing bacteria, such as Gammaproteobacteria_Incertae_Sedis, KF_JG30_C25, and Solirubrobacterales, which contribute to P-recycling in acid soil. AcP, acid phosphatase activity; AlP, alkaline phosphatase activity; Sol-P, easily soluble P; Al-P, aluminum bound P; Fe-P, iron bound P; Ca-P, calcium bound P.

B12−WMSP1 and Solirubrobacterales were significantly enriched in soybean rhizosphere (Fig. 2-E). Among these, the abundance of KF−JG30−C25, Salinisphaerales, Gammaproteobacteria_Incertae_Sedis, Chthonomonadales, B12−WMSP1, and Solirubrobacterales exhibited significant positive correlations with rhizosphere citrate or/and oxalate concentration (Fig. 2-F). Since organic acid secretion can modulate plant rhizosphere microorganism communities (Wen *et al.* 2020; Sindhu *et al.* 2022; Wang *et al.* 2023; Zhang *et al.* 2023), these bacterial genera may be attracted by soybean root-exudated citrate and oxalate. These results strongly indicate that P-deficiency-induced soybean root organic acid exudation may facilitate the recruitment of specific rhizobacteria associated with P acquisition in P-deficient acid soils.

4.2. *GmSTOP1-3* overexpression changes soybean root organic acid secretion and rhizosphere bacterial community

To validate the role of soybean-exuded oxalate and citrate in enriching specific bacterial taxa, transgenic soybean plants with *GmSTOP1-3*-overexpressing were selected for further analysis (Liu G X *et al.* 2024, 2025). As a member of the STOP1 transcription factor family, *GmSTOP1-3* serves a crucial role in plant adaptation to multiple acid soil syndromes, including proton stress, Al toxicity, and P deficiency (Zhou *et al.* 2018; Ye *et al.* 2021; Li and Tian 2023; Liu *et al.* 2025). Previous research has demonstrated that *STOP1* family genes regulate the transcripts of *MATE* transporter genes that facilitate citrate excretion from roots in numerous plant species (Liu *et al.* 2009; Kobayashi *et al.* 2014; Li and Tian 2023; Liu *et al.* 2025). This study revealed that overexpression of *GmSTOP1-3* substantially increased the expression of two *MATE* genes (Fig. 3-B). The enhancement of these genes corresponded with the higher rhizosphere citrate concentration of *GmSTOP1-3*-overexpressing soybean plants (Fig. 3-E). Beyond the *MATE* genes, *GmSTOP1-3* overexpression also increased the expression of two genes encoding OT channels (Fig. 3-B). The OT gene family has been shown to mediate oxalate secretion in Arabidopsis and rubber tree (*H. brasiliensis*) (Yang *et al.* 2022, 2023). The higher oxalate concentration in the rhizosphere of *GmSTOP1-3*-overexpressing soybean plants strongly suggested that *GmOT1* and *GmOT2* might respond to the increased root oxalate secretion (Fig. 3-D). These results establish *GmSTOP1-3*-overexpressing transgenic soybean plants as suitable plant material for simulating soybean wild type plants under P-deficiency conditions.

To elucidate the relationship between root-exuded organic acid and rhizosphere bacteria composition, rhizosphere bacterial community diversity of WT and OX plants was subsequently compared. Results showed that the Simpson and Shannon indices of the rhizosphere bacterial community of OX were significantly higher than those of WT (Fig. 4-A). It is not surprising that increasing soil carbon content could stimulate the growth of microorganisms (Wen *et al.* 2020; Meng *et al.* 2022). For example, the exogenous addition of organic acids, such as citric, malic, tartaric, and oxalic acid, significantly increased the Chao1 index and Shannon index in *Kandeliaobovata* rhizosphere soils (Meng *et al.* 2022). Specific root exudated organic acids have been demonstrated to stimulate the growth of some special microorganisms (Wen *et al.* 2020; Wang *et al.* 2023; Zhang *et al.* 2023). Citric acid and malic acid in watermelon (*Citrullus lanatus*), oxalic, malic and fumaric acid in banana (*Musa paradisiaca*), citric acid, pyruvate acid, succinic acid, and fumarate in cucumber (*Cucumis sativus*) are important significant inducers of *Paenibacillus*, *Bacillus*, and Comamonadaceae, respectively (Ling *et al.* 2011; Yuan *et al.* 2015; Wen *et al.* 2020). A recent study also reported that the relative abundance of *Pseudomonas* and *Bacillus* in lemon tree rhizosphere positively correlated with the increased oxalic acid concentration in acid soil (Wang *et al.* 2023).

To investigate which bacteria are attracted by oxalate and citrate exuded from soybean roots, Metastats analysis was performed to compare the bacterial community composition between WT and OX plants. The analysis revealed significant enrichments of 19 bacterial orders in the rhizosphere of OX plants compared to WT (Fig. 5-A). Among these, Gammaproteobacteria_Incertae_Sedis, KF_JG30_C25 and Solirubrobacterales were identified as bacterial orders that coincided with those enriched in P-deficient soybean rhizosphere (Fig. 5-B). Furthermore, the relative abundances of these three bacterial orders demonstrated significant positive correlations with rhizosphere citrate and oxalate concentrations (Fig. 5-C). This indicates that increased oxalate and citrate accumulation attracts similar bacteria as those enriched in P-deficient soybean rhizosphere, even in P-sufficient soils. Thus, soybean modifies bacterial community structures through enhanced oxalate and citrate secretion in P-deficient acid soils.

4.3. Overexpression of *GmSTOP1-3* enhanced soybean rhizobacterial P cycling potential

Soybean tends to utilize organic P-sources in P-deficient acid soils, primarily depending on AcP and AlP derived from organic-P solubilizing microorganisms (Tian *et al.* 2021; Chen *et al.* 2024). This study demonstrated that the OX plant exhibited elevated rhizosphere AcP and AlP activities, while showing reduced concentrations of rhizosphere Al-P, Fe-P, organic P, and total P (Figs. 3-F; Appendix K). Spearman correlation analysis indicated that the relative abundances of three bacteria taxa, Gammaproteobacteria_Incertae_Sedis, KF_JG30_C25 and Solirubrobacterales, correlated positively with rhizosphere AcP and AlP activities (P<0.05), but negatively with rhizosphere Al-P, Fe-P, organic P and total P concentrations (P<0.05) (Fig. 5-D). The reduced rhizosphere Al-P and Fe-P concentrations may result from either direct effects of enhanced root exudation of citrate and oxalate, or indirect effects of rhizosphere microorganisms (Gomez-Zepeda *et al.* 2021; Sindhu *et al.* 2022; Wang *et al.* 2023; Zhang *et al.* 2023). Conversely, the decreased organic-P fraction appears to relate exclusively to increased AcP and AlP activities (Tian *et al.* 2021; Chen *et al.* 2024; Wan *et al.* 2025). Among these bacterial taxa, Solirubrobacterales has been established as a contributor to P-dissolving in

acid soils (Wang *et al.* 2022; Xie *et al.* 2024). Additionally, Gammaproteobacteria_Incertae_Sedis and KF_JG30_C25 belong to Proteobacteria, a dominant phylum of *phoC*/*phoD*-harboring microbes involved in organic-P mineralization (Luo *et al.* 2019; Chen *et al.* 2024). These findings suggest that OX plants may recruit these specific rhizobacteria for rhizosphere P forage. The Gammaproteobacteria_Incertae_Sedis, KF_JG30_C25 and Solirubrobacterales likely play significant roles in soybean utilization of sparingly soluble P sources in P-deficient acid soil.

Microbial P-transformation processes are primarily governed by four microbial gene categories, including organic P-mineralization genes (e.g., *olpA*, *phoN*, *phoAB*, *phoD* and *appA*), inorganic P-solubilization genes (e.g., *ppa*, *ppk*, *ppx*, *gcd* and *pqqABCDE*), P-uptake and transport genes (e.g., *PstSCAB*, *pit* and *pitAB*), and P-starvation response regulation genes (e.g., *phoB*, *phoR* and *phoU*) (Bergkemper *et al.* 2016; Dai *et al.* 2020; Liu *et al.* 2023). This study demonstrated that the relative abundances of organic P-mineralization genes (*olpA*, *phoAB*, *phoD* and *appA*) and inorganic P-solubilization genes (e.g., *ppk* and *ppx*) were elevated in OX plants (Fig. 6-A). These organic-P and inorganic-P recycling genes exhibited positive correlations with rhizosphere oxalate and citrate concentrations, AcP and AlP activities, while showing negative correlations with Fe-P, Al-P and organic-P concentrations (Fig. 6-B and C). These findings underscore the essential role of microbial P-transformation processes in soybean rhizosphere P recycling. Additionally, these organic P-mineralization and inorganic P-solubilization genes enriched in the rhizosphere of OX plants demonstrated positive correlations with the relative abundances of Gammaproteobacteria_Incertae_Sedis, KF_JG30_C25 and Solirubrobacterales (Fig. 6-D). Consequently, Gammaproteobacteria_Incertae_Sedis, KF_JG30_C25 and Solirubrobacterales appear to be the predominant bacterial orders facilitating P remobilization in the soybean rhizosphere.

5. Conclusion

The evidence indicates that in acid soils with low Pi-availability, transcription factor *GmSTOP1-3* plays a vital role in regulating soybean root citrate and oxalate exudations, which simultaneously recruits and enriches phosphate-solubilizing bacteria, such as Gammaproteobacteria_Incertae_Sedis, KF_JG30_C25 and Solirubrobacterales. These specialized bacteria enhance soybean rhizosphere P-recycling through the activation of organic P-mineralization and inorganic P-solubilization genes (Fig. 6-E). This study emphasizes the significance of root-exuded oxalate and citrate in shaping soybean rhizosphere bacterial community composition and P utilization in P-deficient acid soils. Future studies will systematically validate the organic-P mineralization capacity of these phosphate-solubilizing bacteria in the soybean rhizosphere by inoculation experiments.

Acknowledgements

This work was supported by National Key Research and Development Program of China (2021YFF1000500), the National Science and Technology Innovation 2030 Major Program, China (2023ZD04072), the Guangdong Basic and Applied Basic Research Foundation, China (2025A1515012159).

Declaration of competing interest

The authors declare that they have no conflict of interest.

Declaration of generative AI and AI-assisted technologies in the writing process

During the preparation of this manuscript, the authors used Deepseek to assist in improving the clarity and readability of the language. All content generated was carefully reviewed and revised by the authors as necessary, and the authors take full responsibility for the final content of the article.

Appendices associated with this paper are available at https://doi.org/10.1016/j.jia.2025.08.015

References

Aallam Y, Dhiba D, Lemriss S, Souiri A, Karray F, El Rasafi T, Saïdi N, Haddioui A, El Kabbaj S, Virolle M J, Hamdali H. 2021. Isolation and characterization of phosphate solubilizing *Streptomyces* sp. endemic from sugar beet fields of the Beni-Mellal region in Morocco. *Microorganisms*, **9**, 914.

Balzergue C, Dartevelle T, Godon C, Laugier E, Meisrimler C, Teulon J M, Creff A, Bissler M, Brouchoud C, Hagège A, Müller J, Chiarenza S, Javot H, Becuwe-Linka N, David P, Péret B, Delannoy E, Thibaud M C, Armengaud J, Abel S, *et al.* 2017. Low phosphate activates STOP1-ALMT1 to rapidly inhibit root cell elongation. *Nature Communications*, **8**, 15300.

Bergkemper F, Schöler A, Engel M, Lang F, Krüger J, Schloter M, Schulz S. 2016. Phosphorus depletion in forest soils shapes bacterial communities towards phosphorus recycling systems. *Environmental Microbiology*, **18**, 1988–2000.

Bremner J M, Mulvaney C S. 1982. Nitrogen-total. In: Page A L, Miller R H, Keeney D R, eds., *Methods of Soil Analysis*. Soil Science Society of America, American Society of Agronomy, Madison. pp. 595–617.

Carvalhais L C, Dennis P G, Fedoseyenko D, Hajirezaei M R, Borriss R, von Wirén N. 2011. Root exudation of sugars, amino acids, and organic acids by maize as affected by nitrogen, phosphorus, potassium, and iron deficiency. *Journal of Plant Nutrition and Soil Science*, **174**, 3–11.

Chang S C, Jackson M L. 1957. Fractionation of soil phosphorus. *Soil Science*, **84**, 133–144.

Chen Q Q, Wu W W, Zhao T, Tan W Q, Tian J, Liang C Y. 2019. Complex gene regulation underlying mineral nutrient homeostasis in soybean root response to acidity stress. *Genes*, **10**, 402.

Chen Q Q, Zhao Q, Xie B X, Lu X, Guo Q, Liu G X, Zhou M, Tian J H, Lu W G, Chen K, Tian J, Liang C Y. 2024. Soybean (*Glycine max*) rhizosphere organic phosphorus recycling relies on acid phosphatase activity and specific phosphorus-mineralizing-related bacteria in phosphate deficient acid soils. *Journal of Integrative Agriculture*, **23**, 1685–1702.

Chen X D, Jiang N, Condron L M, Dunfield K E, Chen Z H, Wang J K, Chen L J. 2019. Impact of long-term phosphorus fertilizer inputs on bacterial *phoD* gene community in a maize field, Northeast China. *Science of the Total Environment*, **669**, 1011–1018.

Chen X H, Yan X J, Wang M K, Cai Y Y, Weng X F, Su D, Guo J X, Wang W Q, Hou Y, Ye D L, Zhang S W, Liu D H, Tong L, Xu X Z, Zhou S G, Wu L Q, Zhang F S. 2022. Long-term excessive phosphorus fertilization alters soil phosphorus fractions in the acidic soil of pomelo orchards. *Soil & Tillage Research*, **215**, 1–15.

Chen Z C, Liao H. 2016. Organic acid anions: An effective defensive weapon for plants against aluminum toxicity and phosphorus deficiency in acidic soils. *Journal of Genetics and Genomics*, **43**, 631–638.

Dai Z M, Liu G F, Chen H H, Chen C R, Wang J K, Ai S Y, Wei D, Li D M, Ma B, Tang C X, Brookes P C, Xu J M. 2020. Long-term nutrient inputs shift soil microbial functional profiles of phosphorus cycling in diverse agroecosystems. *ISME Journal*, **14**, 757–770.

Douglas G M, Maffei V J, Zaneveld J R, Yurgel S N, Brown J R, Taylor C M, Huttenhower C, Langille M G I. 2020. PICRUSt2 for prediction of metagenome functions. *Nature Biotechnology*, **38**, 685–688.

Gao P X, Han R R, Xu H, Wei Y M, Yu Y X. 2024. Identification of MATE family and characterization of *GmMATE13* and *GmMATE75* in soybean's response to aluminum stress. *International Journal of Molecular Sciences*, **25**, 3711.

Godon C, Mercier C, Wang X, David P, Richaud P, Nussaume L, Liu D, Desnos T. 2019. Under phosphate starvation conditions, Fe and Al trigger accumulation of the transcription factor STOP1 in the nucleus of Arabidopsis root cells. *Plant Journal*, **99**, 937–949.

Gomez-Zepeda D, Frausto M, Najera-Gonzalez H R, Herrera-Estrella L, Ordaz-Ortiz J J. 2021. Mass spectrometry-based quantification and spatial localization of small organic acid exudates in plant roots under phosphorus deficiency and aluminum toxicity. *Plant Journal*, **106**, 1791–1806.

Herrera-Estrella L, Lopez-Arredondo D. 2016. Phosphorus: The underrated element for feeding the world. *Trends in Plant Science*, **21**, 461–463.

Isidra-Arellano M C, Delaux P M, Valdés-López O. 2021. The phosphate starvation response system: Its role in the regulation of plant–microbe interactions. *Plant and Cell Physiology*, **62**, 392–400.

Kobayashi Y, Ohyama Y, Kobayashi Y, Ito H, Iuchi S, Fujita M, Zhao C R, Tanveer T, Ganesan M, Kobayashi M, Koyama H. 2014. STOP2 activates transcription of several genes for Al- and low pH-tolerance that are regulated by STOP1 in *Arabidopsis*. *Molecular Plant*, **7**, 311–322.

Kuo S. 1996. Phosphorus. In: Sparks D L, Page A L, Helmke P A, Loeppert R H, eds., *Methods of Soil Analysis.* Part 3. Chemical Methods. Soil Science Society of America, American Society of Agronomy, Madison. pp. 869–919.

Lambers H. 2022. Phosphorus acquisition and utilization in plants. *Annual Review of Plant Biology*, **73**, 17–42.

Li J, Yang Y, Wen J L, Mo F, Liu Y. 2022. Continuous manure application strengthens the associations between soil microbial function and crop production: Evidence from a 7-year multisite field experiment on the Guanzhong Plain. *Agriculture*, *Ecosystems & Environment*, **338**, 108082.

Li X B, Tian Y F. 2023. STOP1 and STOP1-like proteins, key transcription factors to cope with acid soil syndrome. *Frontiers in Plant Science*, **14**, 1200139.

Li X X, Tian J, Chen X P, Liao H. 2024. Bioengineering and management for efficient and sustainable utilization of phosphorus in crops. *Current Opinion in Biotechnology*, **90**, 103180.

Li X X, Zhang X H, Zhao Q S, Liao H. 2023. Genetic improvement of legume roots for adaptation to acid soils. *Crop Journal*, **11**, 1022–1033.

Liang C Y, Wang J X, Zhao J, Tian J, Liao H. 2014. Control of phosphate homeostasis through gene regulation in crops. *Current Opinion in Plant Biology*, **21**, 59–66.

Ling N, Raza W, Ma J H, Huang Q W, Shen Q R. 2011. Identification and role of organic acids in watermelon root exudates for recruiting *Paenibacillus polymyxa* SQR-21 in the rhizosphere. *European Journal of Soil Biology*, **47**, 374–379.

Liu G X, Chen Q Q, Li D Q, Mai H F, Zhou Y M, Lin M X, Feng X N, Lin X Y, Lu X, Chen K, Tian J, Liang C Y. 2025. GmSTOP1–3 increases soybean manganese accumulation under phosphorus deficiency by regulating *GmMATE2/13* and *GmZIP6/GmIREG3*. *Plant*, *Cell & Environment*, **48**, 1812–1828.

Liu G X, Li D Q, Mai H F, Lin X Y, Lu X, Chen K, Wang R T, Riaz M, Tian J, Liang C Y. 2024. GmSTOP1-3 regulates flavonoid synthesis to reduce ROS accumulation and enhance aluminum tolerance in soybean. *Journal of Hazardous Materials*, **480**, 136074.

Liu J P, Magalhaes J V, Shaff J, Kochian L V. 2009. Aluminum-activated citrate and malate transporters from the MATE and ALMT families function independently to confer *Arabidopsis* aluminum tolerance. *Plant Journal*, **57**, 389–399.

Liu J P, Xu W F, Zhang Q, Liao W C, Li L, Chen S, Yang J Y, Wang Z R, Xu F Y. 2024. OsPHR2-mediated recruitment of *Pseudomondaceae* enhances rice phosphorus uptake. *Plant Communications*, **5**, 100930.

Liu L, Gao Z Y, Yang Y, Gao Y, Mahmood M, Jiao H J, Wang Z H, Liu J S. 2023. Long-term high-P fertilizer input shifts soil P cycle genes and microorganism communities in dryland wheat production systems. *Agriculture Ecosystems & Environment*, **342**, 108226.

Luo G W, Sun B, Li L, Li M H, Liu M Q, Zhu Y Y, Guo S W, Ling N, Shen Q R. 2019. Understanding how long-term organic amendments increase soil phosphatase activities: Insight into *phoD*- and *phoC*-harboring functional microbial populations. *Soil Biology & Biochemistry*, **139**, 107632.

Meng H J, Yan Z Z, Li X Z. 2022. Effects of exogenous organic acids and flooding on root exudates, rhizosphere bacterial community structure, and iron plaque formation in *Kandelia obovata* seedlings. *Science of the Total Environment*, **830**, 154695.

Mo X H, Liu G X, Zhang Z Y, Lu X, Liang C Y, Tian J. 2022. Mechanisms underlying soybean response to phosphorus deficiency through integration of omics analysis. *International Journal of Molecular Sciences*, **23**, 4592.

Neumann G. 2006. Quantitative determination of acid phosphatase activity in the rhizosphere and on the root surface. In: Luster J, Finlay R, eds., *Handbook of Methods Used in Rhizosphere Research*. Swiss Federal Research Institute WSL, Birmensdorf. pp. 426–427.

Nizigiyimana P, Xu B Y, Liu L R, Luo L P, Liu T T, Jiang M, Liu Z H, Li C J, Luo X H, Lei M X. 2022. Gut microbiota is associated with differential metabolic characteristics: A study on a defined cohort of Africans and Chinese. *Frontiers in Endocrinology*, **13**, 942383.

Nwoke O C, Diels J, Abaidoo R, Nziguheba G, Merckx R. 2008. Organic acids in the rhizosphere and root characteristics of soybean (*Glycine max*) and cowpea (*Vigna unguiculata*) in relation to phosphorus uptake in poor savannah soils. *African Journal of Biotechnology*, **7**, 3617–3624.

Pang J Y, Bansal R, Zhao H X, Bohuon E, Lambers H, Ryan M H, Ranathunge K, Siddique K H M. 2018. The carboxylate-releasing phosphorus-mobilizing strategy can be proxied by foliar manganese concentration in a large set of chickpea germplasm under low phosphorus supply. *New Phytologist*, **219**, 518–529.

Paries M, Gutjahr C. 2023. The good, the bad, and the phosphate: Regulation of beneficial and detrimental plant-microbe interactions by the plant phosphate status. *New Phytologist*, **239**, 29–46.

Peng W T, Wu W W, Peng J C, Li J J, Lin Y, Wang Y N, Tian J, Sun L L, Liang C Y, Liao H. 2018. Characterization of the soybean *GmALMT* family genes and the function of *GmALMT5* in response to phosphate starvation. *Journal of Integrative Plant Biology*, **60**, 216–231.

Sadeghi E, Nasrabadi R G, Naini S A M, Motlagh M B, Sarmast M K. 2024. Assessing the co-composting of wheat straw: A study on compost quality and phosphorus levels for improved soil biochemical responses and maize growth. *Journal of Soil Science and Plant Nutrition*, **24**, 6248–6267.

Shen J, Rengel Z, Tang C, Zhang F. 2003. Role of phosphorus nutrition in development of cluster roots and release of carboxylates in soil-grown *Lupinus albus*. *Plant and Soil*, **248**, 199–206.

Shen J B, Yuan L X, Zhang J L, Li H G, Bai Z H, Chen X P, Zhang W F, Zhang F S. 2011. Phosphorus dynamics: From soil to plant. *Plant Physiology*, **156**, 997–1005.

Shi J C, Zhao B Y, Zheng S, Zhang X W, Wang X L, Dong W T, Xie Q J, Wang G, Xiao Y P, Chen F, Yu N, Wang E T. 2021. A phosphate starvation response-centered network regulates mycorrhizal symbiosis. *Cell*, **184**, 5527–5540.

Sims J T. 2000. Soil test phosphorus: Bray and Kurtz P–1. In: Pierzynski G M, ed., *Methods of Phosphorus Analysis for Soils*, *Sediments*, *Residuals*, *and Waters*. North Carolina State University, Raleigh. pp. 13–14.

Sindhu S S, Sehrawat A, Glick B R. 2022. The involvement of organic acids in soil fertility, plant health and environment sustainability. *Archives of Microbiology*, **204**, 720.

Tian J H, Kuang X Z, Tang M T, Chen X D, Huang F, Cai Y X, Cai K Z. 2021. Biochar application under low phosphorus input promotes soil organic phosphorus mineralization by shifting bacterial *phoD* gene community composition. *Science of the Total Environment*, **779**, 146556.

Tian J H, Lu X, Chen Q Q, Kuang X Z, Liang C Y, Deng L S, Lin D J, Cai K Z, Tian J. 2020. Phosphorus fertilization affects soybean rhizosphere phosphorus dynamics and the bacterial community in

karst soils. *Plant and Soil*, **475**, 137–152.
Vance C P, Uhde-Stone C, Allan D L. 2003. Phosphorus acquisition and use: Critical adaptations by plants for securing a nonrenewable resource. *New Phytologist*, **157**, 423–447.
Walkley A, Black I A. 1934. An examination of the Degtjareff method for determining soil organic matter and a proposed modification of the chromic acid titration method. *Soil Science*, **37**, 29–38.
Wan W, Gadd G M, Xiong X, Zhang W, Liu W, He D, Cheng Y, Yang Y. 2025. Stronger dispersal potential of alkaline phosphatase-encoding bacteria ensures higher organic phosphorus mineralization rate. *Functional Ecology*, **39**, 756–769.
Wang J L, Liu K L, Zhao X Q, Gao G F, Wu Y H, Shen R F. 2022. Microbial keystone taxa drive crop productivity through shifting aboveground-belowground mineral element flows. *Science of the Total Environment*, **811**, 152342.
Wang Q Q, Sheng J D, Wang Y J, Chen K, Lambers H, Wang X R. 2021. The relative contribution of indigenous and introduced arbuscular mycorrhizal fungi and rhizobia to plant nutrient acquisition in soybean/maize intercropping in unsterilized soils. *Applied Soil Ecology*, **168**, 104124.
Wang Y Y, Luo D H, Xiong Z Y, Wang Z F, Gao M. 2023. Changes in rhizosphere phosphorus fractions and phosphate-mineralizing microbial populations in acid soil as influenced by organic acid exudation. *Soil & Tillage Research*, **225**, 105543.
Wang Z A, Li Q, Ge X Y, Yang C L, Luo X L, Zhang A H, Xiao J L, Tian Y C, Xia G X, Chen X Y, Li F G, Wu J H. 2015. The mitochondrial malate dehydrogenase 1 gene *GhmMDH1* is involved in plant and root growth under phosphorus deficiency conditions in cotton. *Scientific Reports*, **5**, 10343.
Wen T, Yuan J, He X M, Lin Y, Huang Q W, Shen Q R. 2020. Enrichment of beneficial cucumber rhizosphere microbes mediated by organic acid secretion. *Horticulture Research*, **7**, 154.
Wen Z H, Li H B, Shen Q, Tang X M, Xiong C Y, Li H G, Pang J Y, Ryan M H, Lambers H, Shen J B. 2019. Tradeoffs among root morphology, exudation and mycorrhizal symbioses for phosphorus-acquisition strategies of 16 crop species. *New Phytologist*, **223**, 882–895.
Xie H J, Chai Y B, Liu Z Y, Hao W Y, Gai J P. 2024. Community assembly of endophytic bacteria and fungi differs in soil-root continuum of *Carex cepillacea*. *Applied Soil Ecology*, **194**, 105206.
Xu Q, Wang X J, Tang C X. 2019. Rhizosphere priming of two near-isogenic wheat lines varying in citrate efflux under different levels of phosphorus supply. *Annals of Botany*, **124**, 1033–1042.
Yang S Y, Lin W Y, Hsiao Y M, Chiou T J. 2024. Milestones in understanding transport, sensing, and signaling of the plant nutrient phosphorus. *Plant Cell*, **36**, 1504–1523.
Yang Z M, Zhao P J, Luo X H, Peng W T, Liu Z F, Xie G S, Wang M Y, An F. 2023. An oxalate transporter gene, *AtOT*, enhances aluminum tolerance in *Arabidopsis thaliana* by regulating oxalate efflux. *International Journal of Molecular Sciences*, **24**, 4516.
Yang Z M, Zhao P J, Peng W T, Liu Z F, Xie G S, Ma X W, An Z W, An F. 2022. Cloning, expression analysis, and functional characterization of candidate oxalate transporter genes of *HbOT1* and *HbOT2* from rubber tree (*Hevea brasiliensis*). *Cells*, **11**, 3793.
Ye J Y, Tian W H, Zhou M, Zhu Q Y, Du W X, Zhu Y X, Liu X X, Lin X Y, Zheng S J, Jin C W. 2021. STOP1 activates NRT1.1-mediated nitrate uptake to create a favorable rhizospheric pH for plant adaptation to acidity. *The Plant Cell*, **33**, 3658–3674.
Yuan J, Zhang N, Huang Q W, Raza W, Li R, Vivanco J M, Shen Q R. 2015. Organic acids from root exudates of banana help root colonization of PGPR strain *Bacillus amyloliquefaciens* NJN-6. *Scientific Reports*, **5**, 13438.
Zhang F B, Hou Y X, Zed R, Mauchline T H, Shen J B, Zhang F S, Jin K M. 2023. Root exudation of organic acid anions and recruitment of beneficial actinobacteria facilitate phosphorus uptake by maize in compacted silt loam soil. *Soil Biology & Biochemistry*, **184**, 109074.
Zhou Y, Yang Z, Gong L, Liu R K, Sun H R, You J F. 2018. Molecular characterization of *GmSTOP1* homologs in soybean under Al and proton stress. *Plant and Soil*, **427**, 213–230.
Zhu S N, Guo Q, Xue Y B, Lu X, Lai T, Liang C Y, Tian J. 2024. Impaired glycosylation of GmPAP15a, a root-associated purple acid phosphatase, inhibits extracellular phytate-P utilization in soybean. *Plant*, *Cell & Environment*, **47**, 259–277.
Zou T, Zhang X, Davidson E A. 2022. Global trends of cropland phosphorus use and sustainability challenges. *Nature*, **611**, 81–87.

Executive Editor-in-Chief Keke Yi
Managing Editor Lujuan Sun